

# Responses to SSM on Uncertainties in Hydrogeological Calculations, Question 1

**Lee Hartley, AMEC**

**Sven Follin, Golder Associates**

**Jan-Olof Selroos, SKB**

## Background

Question 1 of SSM2011-2426-109 calls for (English translation):

“A discussion on uncertainties in the hydrogeological calculations stemming from calibration, measurement methods, and conceptual models is requested. It should also be reported how these uncertainties are propagated into the safety assessment SR-Site considering key factors of importance for the results of the assessment (e.g., distributions of deposition hole flows, transport resistance, and effect of groundwater flow on geochemical stability in the near-field).”

## Introduction

As explained in Selroos and Follin (2010) hydrogeological analyses were performed in SR-Site not only to support assessments of the groundwater pathway for radionuclide transport, but also assessments of the long-term performance of the buffer as this is conditional on hydraulic and hydrogeochemical conditions in the bedrock. These analyses were typically made using 3D hydrogeological models to calculate the spatial distributions of hydraulic and hydrogeochemical quantities on the basis of detailed site specific conditions defined by the site descriptive model (SDM) of Forsmark at completion of the site investigation phase (SKB 2008). Combined discrete fracture network (DFN) and equivalent continuous porous medium (ECPM) representations of bedrock hydrogeology were used for simulation of post-closure conditions during the temperate climate periods (Joyce et al. 2010a), while ECPM representations were used for excavation /operational conditions (Svensson and Follin 2010) and glacial climate periods (Vidstrand et al. 2010). Although modelling scales and software varied between these studies, hydraulic properties were derived from the same underlying hydrogeological DFN (Hydro-DFN) model (see Chapter 2 of Selroos and Follin 2010). The key hydrogeological properties delivered to SR-Site included:

- Characteristics of the flows around deposition holes, such as equivalent flux ( $U_r$  [ $LT^{-1}$ ]) and equivalent flow rates ( $Q_{eq}$  [ $L^3T^{-1}$ ]);
- Characteristics of the flow-pathways from the deposition holes to surface discharge, such as cumulative advective travel times ( $t_r$  [T]) and flow-related transport resistances ( $F_r$  [ $TL^{-1}$ ]) of particle tracks with the groundwater flow field;

- Characteristics of groundwater composition, given as reference water fractions [-] at a grid of points around the repository at selected times in the immediate temperate period.

The methods used to calculate these quantities are defined in Section 3.2 of Joyce et al. (2010a) and the results obtained are presented in Chapter 6 of Joyce et al. (2010a). How these results were used in SR-Site is detailed in SKB (2011), and Salas et al. (2010) in the case of hydrogeochemical results. Calculating the above hydrogeological inputs to safety assessment required the development of a novel multi-scale modelling methodology, which is described in Chapter 3 of Joyce et al. (2010a), and previously peer reviewed as part of SR-Can (SKB 2006a, Hartley et al. 2006); the algorithms used are summarised in a peer reviewed journal article (Hartley and Joyce 2013).

The derivation of the Hydro-DFN model for Forsmark is explained in Follin et al. (2007a), which also describes the conceptual model, site data used to support the models and their calibration. The approach used to interpret the data and construct the Hydro-DFN model has been deliberately restricted to only use the single-hole fracture characterisation information (borehole image, BIPS; borehole core structural analysis; and Posiva Flow Logging, PFL). The derived Hydro-DFN model combined with the deformation zone model defines the hydrogeological parameterisation of the bedrock. In this way, the additional site hydrogeological and hydrogeochemical data (head measurements, cross-hole pressure interference and groundwater composition data) provides a means to independently confirm that this parameterisation can be applied in predicting wider groundwater flow and solute transport characteristics of the site (Follin et al. 2007b). This so called “confirmatory testing” provided a basis for building confidence in the developed parameterisation, fine-tuning it, measure if some model variants performed better than others, test the sensitivity to assumptions, and integrate hydrogeology with other aspects of site understanding such as hydrogeochemistry and climate evolution (Follin and Hartley 2013). Three peer reviewed journal articles are available that summarise: 1) the transmissivity model for deformation zones used for the site hydrogeological description zones in fractured crystalline rock and analyse its possible correlation to in situ stress (Follin and Stigsson 2013), 2) the DFN modelling approach used for the site hydrogeological description (Follin et al. 2013), and the approaches employed to confirmatory testing of a groundwater flow model used for the site hydrogeological description (Follin and Hartley 2013).

Due to the heterogeneous nature of the hydrogeological system at Forsmark inherent in crystalline rock, the hydraulic properties at every location cannot be uniquely determined from site data. Still, the additional site hydrogeological and hydrogeochemical data did provide constraints on both deformation zone properties and the Hydro-DFN, see Section 3.7 of Follin et al. (2008) for a summary or Chapters 5 and 6 of Follin et al. (2007b) for details. The significant findings from the confirmatory testing for the Hydro-DFN parameterisation were that site conditions were well described although vertical hydraulic communication should be reduced (thus increasing the hydraulic anisotropy), a characteristic not necessarily resolved in the PFL tests of flow towards vertical holes, which lead to the adoption of an alternative fracture set and orientation interpretation in Stage 2.3 of the SDM and SR-Site (see Section 11.6 of Follin et al. (2007a) and Subsection 3.4.3 of Follin et al. (2008)).

The methodology used to interpret the single-hole fracture data to inform the conceptual model and calibrate the Hydro-DFN has developed and been elaborated through a

sequence of studies associated with the phases of site investigations at Forsmark and Laxemar, additional studies to support safety assessment, the site investigations and safety assessments at Olkiluoto, and as part of the ongoing Research, Development and Demonstration programme (SKB 2010). Initial ideas were implemented for a few boreholes as part of Stage 1.2 of the SDM (Hartley et al. 2005, Follin et al. 2005). It was extended to deal with the larger number of boreholes available in Stage 2 of the SDM at Forsmark (Follin et al. 2007a) and the SDM at Laxemar (Rhén et al. 2008). The approach was elaborated to more closely represent conditions observed in individual boreholes (e.g. account for the effects of nearby or intersecting deformation zones, and multiple fracture domains) for safety assessment analyses for Laxemar (Joyce et al. 2010b). Further elaborations were made for the Olkiluoto SDM 2011 to allow for single-hole fracture data from pilot holes drilled underground ahead of the ONKALO facility, as well as considering additional conceptual alternatives and lateral variations in flow conducting fracture intensity (Hartley et al. 2012a). Additional conceptual issues such as calibration of Hydro-DFN models including in-plane heterogeneity were considered in support of the TURVA safety assessment for Olkiluoto (Hartley et al. 2012b). How models can be constrained by underground investigations from tunnel mapping and hydraulic tests is a current focus for research. A peer reviewed journal article (Follin et al. 2013) is available that summarises the DFN modelling for the site hydrogeological description.

In addition, the Hydro-DFN model is founded on more general concepts developed to describe the structural geology of crystalline sites (Munier et al. 2003, Munier 2004) and as applied to Forsmark (Fox 2007). Therefore, in order to discuss and assess the significance of sources of uncertainty such as conceptual uncertainties, and uncertainties relating to model calibration, then it is appropriate to draw upon a wider body of work beyond that specific to the Forsmark Hydro-DFN used in SR-Site. A synthesis of the conceptual framework including the close relationship to structural geology, the DFN modelling methodology as applied to site hydrogeology at Forsmark and Laxemar, supporting studies and the wider literature, and a discussion of recognised uncertainties has been prepared in Hartley and Roberts (2013). In that report, Section 3.4 lists the main assumptions used in DFN modelling; Section 4.7 lists identified uncertainties in Hydro-DFN modelling and their status in terms of how they have been addressed or are regarded; Sections 7.4 and 7.5 give a summary of the uncertainties and their treatment specific to SR-Site; and, Section 8.3 summarises the ongoing treatment of uncertainties, more recent support studies, and possible future approaches. Hence, Hartley and Roberts (2013) provides a background reference that may go some way to addressing the broad essence of the authority's question on uncertainties.

The specific uncertainties that the authority raise are discussed below point-by-point. For each point, the specific comment/question raised by the authority is listed first (taken from Begäran om komplettering SSM2011-2426-109; it is noted that in the questions, for consistency with current SKB terminology we have changed 'GeoDFN' to 'Geo-DFN', 'HydroDFN' to 'Hydro-DFN', and 'HCD' and 'hydraulic conductor domains' to 'deformation zones'). References specific to Forsmark are of course most relevant to these discussions; however, the very nature of the crystalline bedrock at Forsmark makes it difficult to perform extensive statistical analyses, which is where findings from other site investigations can provide some additional insight. The notable characteristics of Forsmark are the extremely low conductive fracture frequency at repository depth, or in conventional hydrogeological terms, a very low bulk hydraulic conductivity. This offers exceptionally favourable conditions for maintaining long-term

integrity of the engineered barrier system, but inhibits the surface based acquisition of extensive hydrogeological databases with which to parameterise stochastic models for the deep bedrock short of excessive drilling. For these reasons references are also given to studies made at the Laxemar and Olkiluoto sites as they provide additional supporting evidence and where more extensive use of stochastic modelling has been possible.

## Data uncertainties

### 1. Posiva flow log's (PFL) measurement accuracy

*Comment/question: The Posiva flow log's (PFL) measurement accuracy in relation to the range of fracture transmissivities represented by the Hydro-DFN model in the nearfield of the repository and its sensitivity to non-ideal conditions. The measurement accuracy of the PFL method has been evaluated through comparisons to tests using the so-called pipe-string system (PSS, e.g., Figure 8-13 in SKB, 2005), but SKB has not presented or referred to any analysis of errors that could result from very low flows in combination with pressure losses in the pipes used to transmit flows from the deeper parts of the borehole, or from leakage through the disks separating the measurement section in the case of damaged rock.*

#### Response

Below, we summarise the methodology for single-hole hydraulic testing applied by SKB at Forsmark and Laxemar. Second, we comment some of the conclusions drawn by Ahokas et al. (2013), who recently examined some of the issues that have been considered to be important for the evaluation of the PFL results recorded in 57 cored boreholes drilled at the Olkiluoto site. The issues considered by Ahokas et al. (2013) are: 1) very low flows including noise, 2) leakages between the rubber discs and the borehole wall, and 3) head losses over the flow meter. The bottom line of the assessment by Ahokas et al. (2013) is that there are different types of potential errors, the magnitudes of which are highly dependent on 1) the in situ conditions in the borehole, and 2) how the PFL measurements are operated. In this regard the PFL method is no different than the PSS method. Based on the P reports that describe the PFL measurements conducted at Forsmark, the conditions at Forsmark are favourable and the operations of the PFL measurements of high quality.

#### *The methodology for single-hole hydraulic testing*

One source of uncertainties associated with hydraulic properties used in the hydrogeological models arises from the detection limit of equipment used in the hydraulic tests. The two types of hydraulic data used for the deep bedrock: PFL-f tests (long duration, short interval, and abstraction) and PSS tests (short duration, longer intervals, and injection) provide a measure of the sensitivity to detection limits and the test configurations used. Figure 1 demonstrates a principal difference between the two test methods with regards to the flow regimes; the operation of the PFL method implies quasi steady-state radial-cylindrical flow to a line sink, whereas the operation of the PSS test method implies transient radial-spherical flow from a point source, particularly if the straddle interval is short.

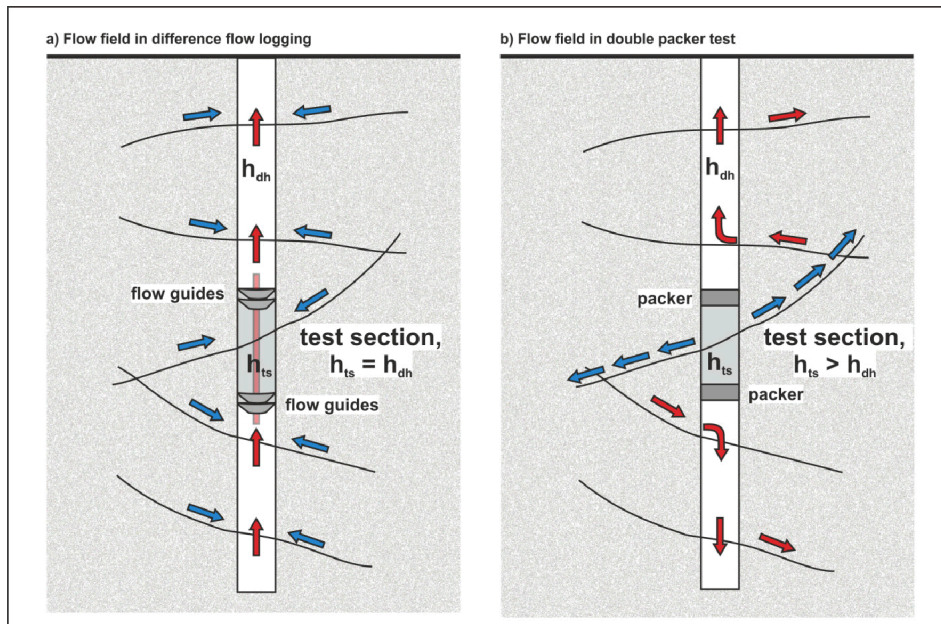


**Figure 1.** Flow field around the drillhole and the test section in a) flow logging and b) PSS tool using a double-packer to isolate the test section (after Ahokas et al. 2013).

The detection limit of the PFL-f method varies depending on the in situ conditions and the way the PFL measurement device is operated (see e.g. Ahokas et al. 2013). Examples of disturbing conditions are floating drilling debris and gas bubbles in the borehole water, or high flow rates (above about 30 L/min) along the borehole. As a rule of thumb, the lower detection limit of the flow meter device used is approximately 30 mL/h ( $8.3 \cdot 10^{-9} \text{ m}^3/\text{s}$ ). The upper detection limit is 300 L/h ( $8.3 \cdot 10^{-5} \text{ m}^3/\text{s}$ ). Typically a drawdown of 5-10m is used implying a range of transmissivities measured between about  $10^{-9}$  to  $10^{-5} \text{ m}^2/\text{s}$ .

For the PSS method, the accuracy of the flow rate measurements depends on the actual flow rate. As a rule of thumb, the lower detection limit of the PSS flow meter device used is approximately 60 mL/h ( $1.7 \cdot 10^{-8} \text{ m}^3/\text{s}$ ), defining the measurement limit for flow. The upper limit for pumping is about 40 L/min. First the tests employing 100 m test sections were performed. For 100 m test-sections showing flow rates above the measurement limit for the flow, tests with 20 m test sections were performed. Subsequently, the tests with a test section length of 5 m were performed for those 20 m test sections showing flow rates above the measurement limit for flow. For a typical injection pressure corresponding to 20 m head, the detection limit means that transmissivities of borehole sections above approximately  $7 \cdot 10^{-10}$  /  $9 \cdot 10^{-10}$  /  $1 \cdot 10^{-9} \text{ m}^2/\text{s}$  are observed for test scales 5 / 20 / 100 m, respectively. Due to the short duration of this type of test, a transmissivity may also be interpreted for isolated fractures, or isolated clusters of fractures, connected to the test section that would not be expected to yield a value for the longer duration PFL tests. Hence, it is important to note that the PSS method may yield an apparent higher number of borehole sections with flow.

For both Forsmark (Follin et al. 2007a, Chapter 4) and Laxemar (Rhén et al. 2008, Chapter 4), consistency between the two types of hydraulic tests was demonstrated by comparing the interpreted total transmissivity values for the same 5m borehole intervals where both types of measurement had been performed. The interpreted values typically falling within an order of magnitude envelope of a 1:1 correlation, although a slight bias

toward higher values in the PSS data was observed (see Figure 4-18 of Follin et al. 2007a) and becoming more apparent at transmissivities below about  $10^{-8}$  m<sup>2</sup>/s. This difference was further examined by quantifying the cumulative distributions of the number of 5m interval transmissivity above different magnitudes (see Table 4-4 and Figure 4-19 of Follin et al. 2007a). The distributions were very similar for values above  $10^{-8}$  m<sup>2</sup>/s. PFL-f tests indicated that 8.1% of 5m intervals had transmissivities above  $10^{-8}$  m<sup>2</sup>/s against 9.6% for PSS; 11% versus 17% above  $10^{-9}$  m<sup>2</sup>/s; and, 14% versus 20% above the respective detection limits. It is not clear which method best reflects actual flow conditions around and below  $10^{-9}$  m<sup>2</sup>/s; however the two methods provide consistent indication that only a small minority, 11-17% of 5m borehole intervals conduct flow above  $10^{-9}$  m<sup>2</sup>/s, provide a consistent bulk hydraulic conductivity and distribution of the flow magnitudes of most concern to safety assessment. The significance of this uncertainty is discussed below (see Point 2 below).

The small number of flowing fractures observed at Forsmark is corroborated by the large number of unbroken 3-m core sticks acquired during the core drillings, see Figure 2. In Figure 3, the data shown in Figure 4-18 of (Follin et al. 2007a) are divided with regard to deformation zones and fracture domains. Figure 3 suggests higher transmissivities are generally associated with deformation zones.



**Figure 2.** More than two-hundred, 3-m long, unbroken core sticks were acquired at depth during core drillings, which support the hydraulic observation of few flowing fractures in the deeper bedrock.

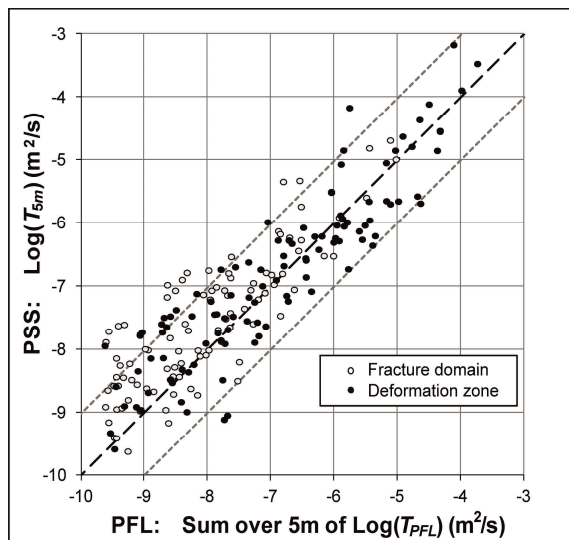


**Figure 3.** Cross plot of 211 five-meter long test sections with both PSS and PFL data above  $1 \cdot 10^{-10} \text{ m}^2/\text{s}$  (cf. Figure 4-18 in Follin et al. 2007a). The data are here divided with regard to deformation zones and fracture domains.

*Very low flows and noise (text based on Ahokas et al. 2013)*

The lower limit of the presently used method is 30 mL/h. A flow of 30 mL/h and a drawdown of 10 m render a specific capacity (“PFL transmissivity”) of about  $10^{-9} \text{ m}^2/\text{s}$ . Significantly greater drawdowns may cause additional head losses due to turbulent flow, see e.g. Ludvigson et al. (2002). However, the resolution of the flow meter device is not the only important factor in optimising the method; the logging speed also has to be taken into account. Thus, the knowledge of low flows is more experimental than theoretical. The practical lower limit of the flow rate is typically determined by calibration, which is done by the operator.

Occasionally there is “noise” in the flow rate making the actual lower limit of the flow meter device higher than 30 mL/h. Examples of disturbing conditions are floating drilling debris and gas bubbles in the borehole water (especially in tunnel work), changes in the salinity of water, a rough borehole wall (especially in percussion drilled boreholes). In such cases the actual lower limit is estimated in the results, which is done by the operator.

Comment: In general, the borehole conditions for PFL measurements were excellent at Forsmark, see e.g. the conclusions in Rouhiainen and Pöllänen (2003): “The base level of flow (lower measurement limit) was low. This usually indicates that the borehole and fracture system is well cleaned from drill cuttings”. Figure 3 reveals that PFL transmissivities with magnitudes lower than  $10^{-9} \text{ m}^2/\text{s}$  were observed in several boreholes at Forsmark. PFL transmissivities of the low-flowing fractures are generally reported as “uncertain” in SKB’s database Sicada. Nevertheless, from a discrete fracture network modelling point of view they were accounted for as their contribution to the conductive fracture frequency is important in sparsely fractured rock.

*Head losses due to leakage around the rubber discs and flow through the bypass tubing  
(text based on Ahokas et al. 2013)*

The diameter of the bypass tubing inside the PFL flow logging device is as wide as possible to minimize possible head losses because of flow along the borehole. The diameter is not possible to change without a rebuild.

Leakage around the rubber discs occurs in almost every borehole because water always tries to find the easiest way to flow, no matter whether the flow rate is low or high. However, the problem is generally more common in rock with high fracture frequency, rough boreholes wall (cavities), and at high flow rates to boreholes near open tunnels (see Ahokas et al. 2013, p 12).

Comment: The main reason for conducting the PFL measurements with two different section lengths (5 m and 1 m) is to identify possible leakages. The two results should reasonably fit with each other, i.e. a comparison of the results should reveal where disc leaks are possible (Ahokas et al. 2013). The identification of potential leakages around rubber discs is further improved by conducting PSS measurements (Ludvigson et al. 2007). Most cored boreholes at Forsmark were tested with both methods (see Appendix B in Follin et al. 2007b). The reasons for results shown in Figure 3 are discussed above and in Follin et al. (2011).

At Forsmark, leakages around the rubber discs of the PFL tool were rare in the deeper parts of most cored boreholes. One of the more complicated cored boreholes was KFM03A located in the hanging wall rock of deformation zones ZFMA2 and ZFMF1 (Figure 4). KFM03A intersects several transmissive gently dipping deformation zones. This prohibited the imposed drawdown at the depth of the submersible pump to reach the deeper parts of the borehole. The hydraulic testing with the PFL method in KFM03A was repeated with a modified instrumentation to improve the quality of the acquired data, see Pöllänen and Sokolnicki (2004) for details.

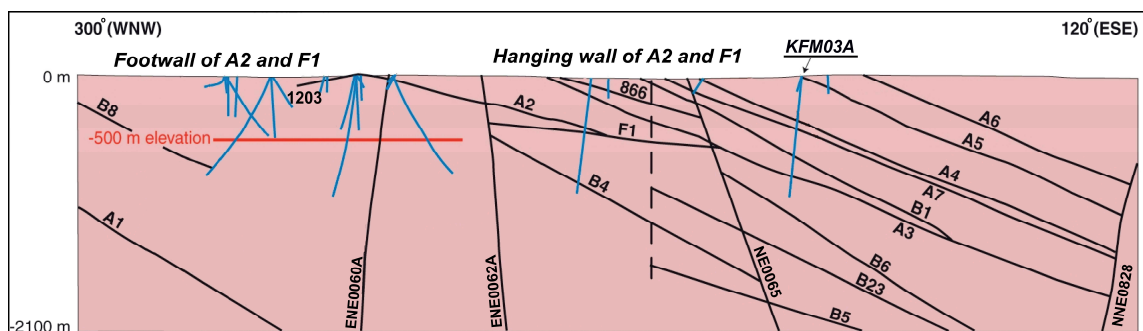


**Figure 4.** WNW-ESE cross-section along the central part of the investigation area at Forsmark. The intersected major deformation zones are shown as solid black lines. The blue lines represent trajectories of core-drilled and percussion-drilled boreholes located in proximity to the cross-section. The location of the c. 1 km deep cored borehole KFM03A is highlighted.

Consequence for SR-Site: Favourable field conditions do not exclude chances for measurement errors, of course, but a systematic bias in the PFL measurements acquired in the target volume is deemed unlikely based on the consistent results reported from 1) the PFL measurements conducted in KFM01A, -01D, -02A, -04A, -05A, -06A, -07A, -07C, -08A, -08C, and -08D, and 2) the corresponding PSS

measurements. The latter data reinforce the perception of a low conductive fracture frequency in fracture domain FFM01 and that the PFL method indeed can identify quite discrete fractures. As an example of the consistent picture provided by these data one can compare the PFL data obtained in KFM04A and KFM07A shown in Figures 4-3 and 5-5 of Follin (2008) with the corresponding PSS data for these two boreholes shown in Figure 5-13 of Follin (2008).

In summary of the discussion above, the conditions at Forsmark are favourable for hydraulic tests using the PFL tool and the operations of the PFL measurements were of high quality. This provided for the base level of flow (lower measurement limit) to be low c.  $10^{-9}$  m<sup>2</sup>/s and sometimes lower. The significance to safety assessment of uncertainties in the intensity and transmissivity of flow conducting fracture intensity below the detection limit is assessed in the next point.

## 2. The sensitivity of model calibration to the PFL's measurement accuracy

Comment/question: The influence of the PFL's measurement accuracy on the calibration of the relationship between fracture size and transmissivity. The PFL measurements used for the calibration are judged to have a measurement accuracy of approximately  $1 \times 10^{-9}$  m<sup>2</sup>/s for the Forsmark rock (Follin et al. 2007, p 38). This is within the same range as the  $Q/s$  values used in the calibration. Particularly interesting in this context is the sensitivity of the calibration in the fracture domain representing volume FFM01 (Follin et al. 2007, p 183, Figure 11-15).

### Response

The Hydro-DFN calibration was mainly focussed on the PFL-f data because of the discrete nature of the measurements lend themselves to interpretation of the hydraulic properties of individual fractures. For example, the differences in properties of different fracture sets can be examined. PSS data was used in some flow calibration targets such as the geometric mean flow to 100m borehole section. Sensitivities to assumptions about flow geometry for a pumping borehole were circumvented by calibrating the simulated specific capacity (inflow/drawdown) directly with that measured, rather than calibrating on so-called PFL fracture transmissivities.

The detection limit of PFL-f tests of specific capacity c.  $10^{-9}$  m<sup>2</sup>/s for surface drilled boreholes is typically a few orders of magnitude lower than geometric mean specific capacity values measured in the upper bedrock (i.e. above -200m elevation at Forsmark), and hence is sufficient to detect flowing features of hydraulic significance. For repository depth, the geometric mean measured transmissivity outside of deformation zones is  $6 \cdot 10^{-9}$  m<sup>2</sup>/s at Forsmark (see Chapter 11 of Follin et al. 2007a), and at Laxemar varies between domains from  $8 \cdot 10^{-9}$  to  $3 \cdot 10^{-8}$  m<sup>2</sup>/s (see Chapter 9 of Rhén et al. 2008). Hence, the detection limit can have an influence on the Hydro-DFN modelling, at least for Forsmark. The Hydro-DFN modelling is essentially only able to calibrate the connected fracture system of fractures with specific capacity above c.  $10^{-9}$  m<sup>2</sup>/s. Based on the comparisons with PSS data discussed under Question 1, one might consider a scenario whereby the intensity of potentially flow conducting fractures is increased by about 50% at depth, i.e. a scaling of 17% for PSS 5m intervals above  $10^{-9}$  m<sup>2</sup>/s compared to 11% for PFL. It would however be pessimistic to apply such a factor across the whole distribution of measured transmissivities. Instead one could consider a scenario whereby 50% more fractures with a PFL transmissivity of c.  $10^{-9}$  m<sup>2</sup>/s were

added to the system in some fashion. The consequences of such a scenario can be estimated by simple analyses.

One simple consequence that could be expected is that more deposition holes would become connected to the system of flow conducting natural fractures, and so have a Q1 path. In SR-Site (Joyce et al. 2010a) this was calculated to be about 24% without filtering on FPC or EFPC, and so this might increase to about 35% (i.e. a 45% increase). The increase in intensity would not be expected to move the whole open fracture system above the percolation threshold, i.e. insufficient to connect all small fractures. The consequences of such extra low transmissivity connections is in many ways already accounted for by the conservative assumption that a continuous EDZ with a transmissivity of  $10^{-8} \text{ m}^2/\text{s}$  (i.e. ten times that of the detection limit for natural fractures) intersects the top of every deposition hole and considering the associated Q2 release path. Nonetheless, the initial equivalent flux for a deposition hole intersected by these low transmissivity natural fractures can be estimated from  $U_r = T\nabla h/d$ , where  $T=1 \cdot 10^{-9} \text{ m}^2/\text{s}$ , the hydraulic gradient perpendicular to the deposition hole is set to a characteristic value for Forsmark of about  $\nabla h = 0.005$  (toward the high-end of values suggested in Figure 6-6 of Follin et al. 2008), and  $d=5\text{m}$  is the canister height, implying a  $U_r$  of about  $3 \cdot 10^{-5} \text{ m/y}$ . The flow-related transport resistance,  $F_r$ , for a pathway through such fractures can be estimated as  $2L/T\nabla h$  with the path distance  $L=500\text{m}$  (approximate distance to the surface or to a deformation zone) to give about  $5 \cdot 10^6 \text{ y/m}$ . For Forsmark, these values are similar to the median values for Q1 paths, which were  $1 \cdot 10^{-5} \text{ m/y}$  for  $U_r$  and  $4 \cdot 10^6 \text{ y/m}$  for  $F_r$ . They are however far lower than in the tails of the performance measures (Joyce et al. 2010a),  $U_r$  of c.  $10^{-2} \text{ m/y}$  and  $F_r$  c.  $10^4 \text{ y/m}$  that might be detrimental for performance of the buffer in the deposition hole and transport of any consequent radionuclide release. The detection limit of the PFL tests is therefore not considered to have a significant effect on long-term safety.

The question of how does the detection limit effect the relationship between the calibrated fracture size and transmissivity relationship has been illustrated directly as part of the Hydro-DFN developed for the Olkiluoto SDM 2011 (Hartley et al. 2012a). There, PFL testing has been performed in 15 pilot holes drilled ahead of the construction of the ONKALO facility at a drawdown similar to the depth of the holes, down to more than 400m depth. The 40 times higher drawdown for these tests implies a 40 times lower detection limit on specific capacity, i.e. c.  $2 \cdot 10^{-11} \text{ m}^2/\text{s}$  compared to  $10^{-9} \text{ m}^2/\text{s}$  for surface drilled holes. The pilot hole measurements confirmed the intensity of flow conducting fractures above  $10^{-9} \text{ m}^2/\text{s}$  detected in surface based investigations, but also revealed additional flow conducting fractures with much lower specific capacity. In fact, the total intensity of such low transmissivity fractures at depth was 6 times that detected from the surface drilled holes. However, the six times higher intensity for a 40 times lower detection limit, as well as the very low magnitudes, implies that these additional fractures have no effect on bulk flow properties above the scale of a few tens of metres. Further, due to staging of the data acquisition, two phases of Hydro-DFN models were derived allowing an objective sensitivity test to the detection limit. The first one without deep pilot holes, essentially using a detection limit of  $10^{-9} \text{ m}^2/\text{s}$ , see Chapter 5 of Hartley et al. (2012a); the second incorporating c. 700m of deep pilot holes, essentially with a detection limit c.  $2 \cdot 10^{-11} \text{ m}^2/\text{s}$ , see Chapter 10 of Hartley et al. (2012a). Fracture intensity-size-transmissivity relationships are derived for each case – compare Tables 5-8 and 10-6, Depth Zone 4. The intensities of PFL fractures are about 6 times higher with the lower detection limit; the coefficients of the transmissivity models are about 40 times lower; and the scaling exponent of transmissivity increases

from 0.4 to 0.7 for semi-correlated and from 0.6 to 1.0 for correlated. In order to calibrate the model against this far more connected system, the size distribution has to be shifted toward more large fractures, and so the shape parameter of the power-law fracture size model also becomes much lower, c. 2.4, with the lower detection limit. This implies the small fractures that were mostly neglected in the surface data derived model become included due to the lower detection, but have a very low transmissivity, while larger fractures remain with similar intensity and transmissivity (cf. Figures 5-13 and 10-2 for effects on size distribution, and Figure 10-6 for transmissivity (Hartley et al. 2012a)). The inclusion of the lower detection limit resulted in Hydro-DFN models that were significantly more connected geometrically giving a higher effective kinematic porosity without a corresponding increase in bulk hydraulic conductivity. Providing hydraulic gradients are not large, the additional connected fractures provide extra volume for free-water diffusion, and extra surface for rock matrix diffusion, which both act to slow solute transport. Upscaled hydraulic conductivities for different model variants based on the lower detection limit were found to be less sensitive to the choice of size-transmissivity model, and had the same geometric mean as for the higher detection limit.

*Consequence for SR-Site: The derived relationships for fracture intensity-size-transmissivity should be considered an appropriate description for the subset of open connected fractures with specific capacities above c.  $10^{-9}$  m<sup>2</sup>/s. If more flow conducting fractures were apparent at a lower detection limit, then the shape factor of power-law size model would become smaller, the coefficient of the size-transmissivity correlation smaller, and the exponent of the size-transmissivity correlation larger. In more practical terms, the connectivity of the system would increase, implying more deposition holes would connect with the natural fracture system and have a Q1 path. However, the flow rates in these fractures would be less than those in the assumed connected EDZ at the top of the deposition hole; estimates of initial equivalent flux would be less than median values calculated in SR-Site, and estimates of flow-related transport resistance would be higher than median values in SR-Site. Therefore, the assessment of the integrity of the engineered barrier system is not considered sensitive to the presence of additional flow conducting fractures below the PFL detection limit. It is noteworthy that such additional low transmissivity fractures would provide an increased surface area for sorption and rock matrix diffusion as well as higher kinematic porosity without significantly affecting bulk hydraulic conductivity, and hence would have some beneficial effects on radionuclide transport calculations. It is expected that a significantly improved quantification of the intensity and distribution of very low specific capacities can only be achieved practically through hydraulic tests performed underground.*

### 3. Is borehole data representative of target area?

*Comment/question: Hydrogeological data has been collected from e.g. boreholes. How has it been accounted for in the consequence calculations, that the data that the hydrogeological calculations are based on, possibly are not fully representative of the real conditions of the target area?*

## Response

In total, 25 core drilled and 38 percussion drilled boreholes were drilled at the site during the site investigations. Even if the different boreholes had different objectives (e.g. to confirm individual deformation zones and volumes in between), they provide a consistent conceptual view of the site. In short, the upper part of the bedrock is highly fractured, whereas the lower part has very few conductive fractures (see also the answers to the question on Conceptual uncertainties below). At the end of the site-investigations, i.e., stage 2.3, a model verification and uncertainty assessment was performed by use of data from an additional five core-drilled and six percussion drilled boreholes not used in the derivation of the previous model version (ver 2.2). This analysis, which is reported in Follin et al. (2008), clearly shows that the conceptual model derived within stage 2.2 is consistent with the additional data collected within stage 2.3. Obviously it could be claimed that also the additional data are biased, but a bias is deemed unlikely (cf. the answer to Question 1) and will ultimately be tested once data collected underground (i.e., from tunnels) will be available.

*Consequence for SR-Site: Based on the discussion above, the uncertainty related to bias in boreholes is deemed negligible.*

## **Conceptual uncertainties**

### 4 Sensitivity to the shape of fractures

*Comment/question: The DFN models are based on fractures that are quadratic or circular as opposed to alternative conceptual assumptions of e.g. elongated fractures possibly leading to sparse networks percolating at lower intensities (Black et al., 2007). A channel network model has been applied by SKB as an alternative to predictions of radionuclide transport (Longcheng et al., 2010), but this model is based on a uniformly connected grid to which properties have been transferred from the Hydro-DFN model.*

## Response

Only the case of square stochastic fractures was considered in the Hydro-DFN modelling since geomechanical mechanisms for the creation of significantly elongated fractures were not apparent. It is possible that elongated flow channels in particular directions could exist within some fractures.

The influence of fracture shape on the connection characteristics of fracture networks has not been studied as part of the site or safety assessment modelling. Some results for elliptical fractures are presented in Black et al. (2007) for uniform fracture size distributions and in de Dreuzy et al. (2000) for power-law fracture size distributions. Black et al. (2007) were motivated by the hypothesis that a network based on ellipses with high aspect ratios, of around 5:1 to 10:1, might provide a better approximation of sparse flow channels than networks of omni-dimensional fractures. The work by de Dreuzy et al. (2000) studied the percolation threshold for the fracture surface area per unit volume required for a network to become connected for a wide variety of power-law shape parameters and eccentricities. It was found that the percolation threshold was relatively insensitive to the eccentricity of fracture ellipses, varying by around a factor 2-3 for fixed shape parameter. The percolation threshold was highest when the eccentricity was between 5:1 to 10:1. Similar conclusions were also made by Mourzenko et al. (2004, 2005).

Our understanding of the significance of the above theoretical studies is that the key parameter to measure at sites to determine hydraulic fracture connectivity is the flow conducting surface area per unit volume (for some threshold on fracture transmissivity suitable to safety assessment, see above), which can be inferred from the fracture intensity (Terzaghi corrected for orientation bias, (Terzaghi 1965)) of flow measurements detected by the PFL method. The same parameter is critical for determining solute transport also as it determines diffusive exchange with the matrix and sorption. Fracture shape is considered to be of secondary importance. It is expected that calibration of model variants including different aspect ratio shapes against observed connectivity and flow distributions in boreholes will yield models with similar connected fracture surface areas per unit volume. This conviction is based on related tests of different fracture size models (different  $r_0$  and  $k_r$ ) for Laxemar (see Section 10.5 of Rhén et al. 2008), testing of power-law versus log-normal size models for Olkiluoto (see Chapter 5 of Hartley et al. 2012a), testing of flow channelling concepts based on chess board style (see Chapter 5 of Hartley et al. 2012a) and variable hydraulic aperture style in-plane heterogeneity (see Section 7.2.4 of Hartley et al. 2012b). These tests cover a wide range of conceptual models including ones affecting the shape of flow channels, albeit not formulated as aspect ratio. In each test it has been found that alternative calibrated DFN conceptual models yield similar distributions of performance measures, such as flows around deposition holes and flow-related transport resistance, although details in the spatial architecture of the flow field can vary.

*Consequence for SR-Site: In summary, it is expected that were alternative DFN models calibrated with different aspect ratios they would yield similar connected fracture surface area per unit volume and performance measures to those applied in SR-Site.*

##### 5. Sensitivity to channelisation of flow within fractures

*Comment/question: The choice of conceptual model for flow through a fracture between channelized or non-channelized flow, with consequences for the interpretation of PFL anomalies and the coupling to fracture size, transmissivity and connectivity.*

##### Response

The variability in specific capacity between fractures observed in the PFL tests (see Chapter 5 of Follin et al. (2007a), for example) is reproduced in models as a consequence of the stochastic nature of the geometry and connectivity of the fractures, essentially giving rise to varying boundary conditions for the flow across individual fractures even without variability in transmissivity between or within fractures. Variability in transmissivity between fractures creates additional variability. These two factors, variations in spatial architecture of the network and in transmissivities between fractures, typically have greater effect than variability within fractures (Painter 2006). For instance, Öhman and Follin (2010) who studied the role of “hydraulic chokes” in a hydrogeological DFN where all fractures had the same transmissivity regardless of fracture size. Öhman and Follin (2010) concluded that in a sparsely fractured model the extent of the geometric contact between two transmissive fractures is crucial for the flow across the contact area; i.e., if the geometric contact was small relative to the size of the two intersecting fractures a “hydraulic choke” occurred.

The precise mix of these effects giving rise to the observed hydraulic variability and the relation to the geometrical properties cannot be inferred. Hence, in the modelling three different assumed size-transmissivity relationships have been considered to quantify the

sensitivity to variability between fractures (see Figure 11-17 of Follin et al. 2007a), for example).

Each of these models can provide sufficient variability to reproduce the observed variability in specific capacity. Differences in flow characteristics between model variants with different size-transmissivity relationships are however apparent in the scale dependence of equivalent hydraulic conductivity (see Figures 5-7 and 5-9 of Hartley and Roberts 2013). For example, the uncorrelated model tends to predict relatively small differences in the geometric mean hydraulic conductivity on the 5m, 20m and 100m scales, while the mean tends to decrease with scale for the semi-correlated and correlated model, which is more consistent with the scale behaviour of the PSS data at both Forsmark and Laxemar. Hence, the uncorrelated model seems less consistent with site data as well as being considered to lack geo-physical motivation, unlike the semi-correlated or correlated models.

Within the Hydro-DFN modelling for SDM-Site and SR-Site, fractures have been represented as planar structures, with constant transmissivity within a fracture. This description reasons that flow at the scales of interest can be adequately represented by the assignment of an effective transmissivity value for a single fracture. This approach has been used for practical reasons because flow channelling cannot be adequately quantified from surface investigations, and models of flow channelling within fractures would therefore be highly speculative. In-plane heterogeneity has been observed in deformation zones where they have been characterised by PFL tests at multiple borehole intersects, and represented by stochastic variations in transmissivity over the zones in SR-Site (see Follin et al. (2007a), Subsection 2.3.3 of Joyce et al. (2010a) and Follin and Stigsson (2013)); the consequence of which is part of the comparison of multiple realisations (Joyce et al. 2010a, Section 6.2.7). However, it was found that performance measures were more sensitive to the generation of large stochastic fractures near the deposition holes than deformation zone heterogeneity. The sensitivity to deformation zone in-plane heterogeneity on simulations of the data used in the confirmatory tests (heads, pressure interference and hydrogeochemistry) is analysed in Section 5.3 of Follin et al. (2008), which showed that the spatial distribution of some species are sensitive to heterogeneity, less so for salinity. This is also described in the peer reviewed journal article by Follin and Hartley (2013).

The hydrogeological system at Forsmark would diverge most from that modelled in SR-Site if flow channels were narrow and sparsely distributed within individual fractures. Under such conditions it would be a concern that PFL hydraulic tests may detect the nearby presence of a flow conduit, but since the borehole is unlikely to intersect it directly then the transmissivity of the structure may be underestimated. This concern has been addressed through analysis of hydraulic tests in boreholes. Generalised radial flow analysis of PSS hydraulic responses in packed off borehole sections at Forsmark (Follin et al. 2011) suggests that most flow-conducting features (70–90%) are associated with flow dimensions greater than 1.5, although a significant minority (10–30%) exhibit smaller flow dimensions characteristic of approximately linear flow channelling. This result is generally consistent with the notion of a hydraulically well connected flow space within the fractures that have been measured. Likewise, generalised radial flow analysis of PSS hydraulic responses in packed off borehole sections at Laxemar (Rhén et al. 2008) suggests that greater than 90% of flow-conducting features on a 5 m test scale are associated with flow dimensions greater than 1.5. Only a limited number of test sections gave indications of approximately linear flow channelling. Given this lack

of evidence for highly channelised flow within fractures, only concepts of variability between fractures have been investigated at Forsmark.

Alternative concepts for channelised flow have been examined in the Hydro-DFN modelling of Olkiluoto. The first alternative was to create a DFN model according to the intensity of all fractures and a power-law size model, as derived from geological DFN modelling, but then restrict the openings on these fractures to only occupy a sub-area of each fracture according to some size dependent probability function (Hartley et al. 2012a). The parameters determining the amount of fracture area that is hydraulically open for a given fracture size was adjusted to mimic the observed fracture connectivity seen in PFL tests. The portion of open surface area being represented on a sub-grid over the fracture surface distributed randomly. The resulting calibrated model restricted the length and area of flow pathways through individual fractures, forcing more tortuous pathways through the 3D network system. The resulting model was found to predict a slightly higher proportion of deposition holes connected to the natural fracture system, but distributions of performance measures for flow rates around deposition holes and flow-related transport resistance were similar to those for the base case Hydro-DFN concept, equivalent to that used in SR-Site (see Subsection 7.2.2 of Hartley et al. 2012b). A second group of alternatives concepts were considered with in-plane variability according to a hydraulic aperture that varied by a few orders of magnitude over each plane such that flow was restricted to only about 30% of the fracture area (see Subsection 5.2.3 and Appendix H of Hartley et al. 2012b). Again, once alternative models were calibrated on the PFL data, resulting predicted distributions of performance measures, e.g.  $U_r$  and  $F_r$ , were consistent between alternative models (see Subsection 7.2.4 of Hartley et al. 2012b).

*Consequence for SR-Site: In summary, it is expected that were alternative DFN models calibrated with greater spatial variability within fractures rather than between fractures then the connected fracture surface area with specific capacity above the PFL detection limit would remain similar to that derived in SDM-Site. The calibration of specific capacity on the PFL flow distribution would also be expected to constrain the predicted distribution of initial equivalent flux around the deposition holes to be similar to that derived in SR-Site. In fact, if heterogeneity is reduced to the scale of individual fractures rather than to the network scale, then the range of initial equivalent fluxes may be narrower. Likewise, flow-related transport resistance would be expected to be largely unchanged since it depends on flow conducting surface area, which can be estimated from PFL fracture intensity, and flow rate, the distribution of which is measured by PFL.*

## 6. Sensitivity to spatial distribution

*Comment/question: The choice of conceptual model for spatial distribution of fractures within the Hydro-DFN model of the hydraulic rock domains, applying a simple Poisson process instead of alternative models that have been developed in the Geo-DFN analysis including fractal scaling, heterogeneous fracture intensities, or influence of deformation zones.*

### Response

The Hydro-DFN model developed for SDM-Site Forsmark focuses on differences between fracture domains that occur on a site scale (see additional information with

regard to sub-domains under bullet 8 below). A Poisson process was adopted for all fracture domains FFM01-FFM06 to describe the spatial distribution of open fractures in 3D on the basis of the geological argumentation in favour of this distribution for all fractures on the scale of tens of meters, see Section 4.3.3 in Fox et al. (2007): “At scales greater than 30 m, the fractures and fracture traces should scale in a Euclidean manner. The scaling exponents are the same for all sets and fracture domains.”

It should be noted that Poissonian spatial structure for “all fractures” (i.e. broken and unbroken) does not imply that the distribution of flow-conducting fractures also exhibits a Poissonian spatial structure, as fractal clustering of such fractures can arise spontaneously in a fracture system if it is close to the percolation threshold, see e.g. (Bour and Davy 1997, 1998, Follin et al. 2006, Appendix C, Hartley and Roberts 2013, Figure 4-18). Furthermore, lack of connectivity implies that the intensity of flow-conducting fractures does not obey the principle of a tectonic continuum at all scales, see Appendix C in Follin (2008).

*Consequence for SR-Site: Since the Geo-DFN analysis concludes that a Euclidean spatial distribution is appropriate at scales greater than 30m, and PFL detected flowing fracture are spaced on the order of a hundred metres or more at repository depth, then there is limited scope or basis for applying alternative spatial models to Hydro-DFN modelling of the deep bedrock. If future hydraulic tests performed underground were to identify more frequent low transmissivity fractures, then alternative spatial models may be more relevant and possibly better supported by e.g. tunnelling mapping.*

## **Uncertainties related to model calibration**

### **7. Sensitivity to interpreted depth trend in deformation zone transmissivity**

*Comment/question: A correlation between transmissivity and depth has been fitted to all deformation zones; this in contrast to a model in which deformation zones with different orientations could have different correlations or perhaps no correlation between transmissivity and depth. The depth dependency is primarily based on data for gently dipping zones (Follin et al., 2007 p 122). For steeply dipping zones, for many of which there is only a single measurement per zone, the application of the derived trend can be questioned. Alternative possibilities such that certain zones would have transmissivities that do not clearly decrease with depth could e.g. have consequences for groundwater flow at great depth and for the possibility of up-coning of very saline waters to repository depth.*

#### Response

A description of the data behind the exponential transmissivity-depth model developed for the deformation zones at Forsmark and an analysis of their potential coupling to the tectonic evolution (geological history) (Stephens et al. 2007) and present-day in-situ stress field (Glamheden et al. 2007, Martin 2007) is provided in the peer reviewed article by Follin and Stigsson (2013). Because the measured stress magnitudes also increase with depth at the Forsmark site it may be hypothesised that the reduction in transmissivity is related to the increase in effective normal stress, see Figure 5 and Figure 6 (cf. Mattila and Tammisto 2012). The plots in Figure 5 and Figure 6 do not falsify the hypothesis that the considerable reduction in the inferred transmissivity data of deterministic deformation zones is partly due to the increasing effective normal stress. This observation includes the steeply dipping deformation zones. However, the

findings of Follin and Stigsson (2013) do not support a notion that the normal stress acting on flowing fractures exclusively controls the magnitude of the flow along the deformation zones at Forsmark. More factors besides stress also affect the calculated transmissivity of deterministic deformation zones, e.g. fracture roughness, variable aperture, poor fracture connectivity, weathering, infill material, etc. Tentatively, laboratory-scale relationships developed from normal stress experiments on a single fracture in crystalline rock (green dashed lines in Figure 5) can be used to estimate the maximum values of transmissivity of the site-scale deformation zones at Forsmark.

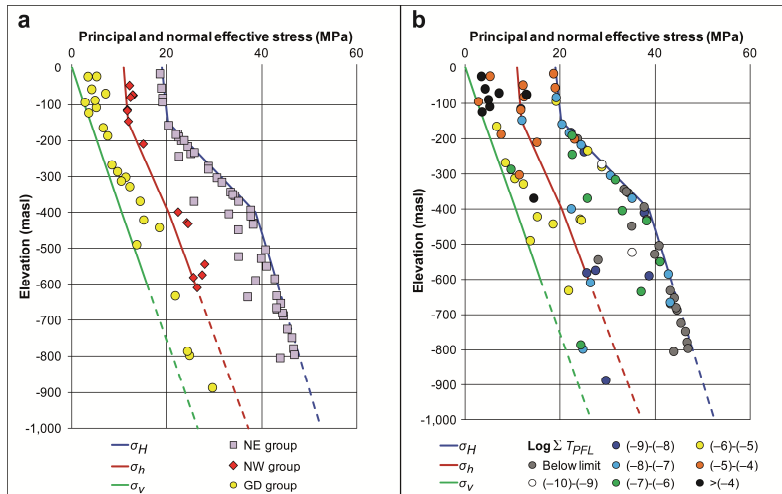


**Figure 5.** Distribution of calculated normal effective stress at the deformation zone intercepts discussed in Follin and Stigsson (2013); **a** According to orientation group, and **b** According to transmissivity. Deformation zone intercepts that do not have measurable flow according to the PFL testing are shown as grey dots in **b**. The principal stresses are taken from Glamheden et al. (2007) and Martin (2007).

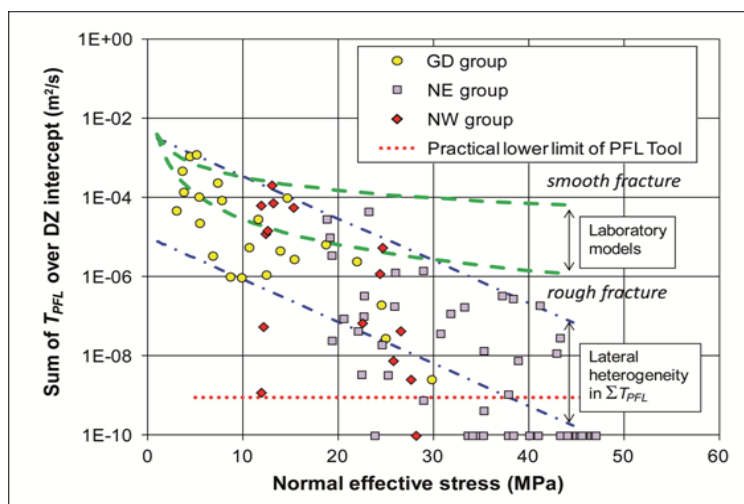


**Figure 6.** Calculated normal effective stress acting on the inferred transmissivity along the plane of the deformation zones. An arbitrary low transmissivity value of  $10^{-10} m^2/s$  is assigned to all deformation zone intercepts that do not have measurable flow according to the PFL testing in order to make them visible in the plot. Reproduced from Follin and Stigsson (2013).

In SDM-Site Forsmark, the observed variation in deformation zone transmissivity with depth was modelled with an exponential model with a conditioned lognormal distribution as a model for the lateral heterogeneity, see Follin et al. (2007a) or Follin and Stigsson (2013) for details. The lateral heterogeneity was included in the confirmatory testing of SDM-Site (see Figure 7-2 of Follin et al. 2008) and in SR-Site (see Figure 4-2 and Section 6.2.7 of Joyce et al. 2010a). Below, we focus on the rationale for an exponential depth trend with strong lateral heterogeneity of the in-plane transmissivity of steeply dipping deformation zones located inside the fracture domain where the proposed repository is located, FFM01, see Figure 7.

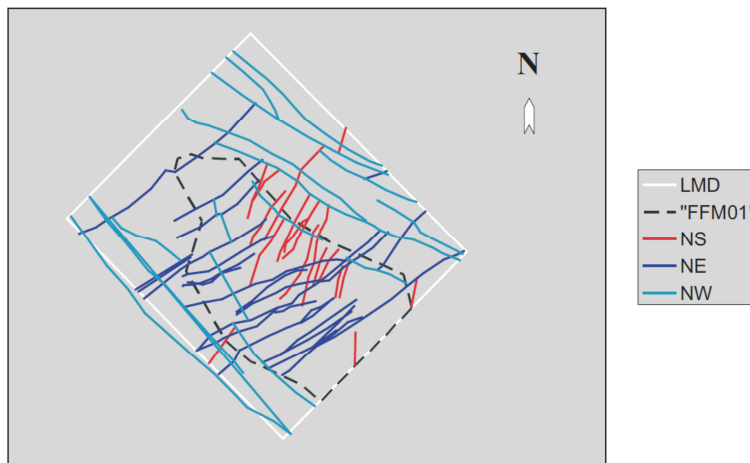


**Figure 7.** Illustration of traces of steeply dipping deformation zones within the local model domain (LMD). The extent of target fracture domain for the repository layout, FFM01, coincides approximately with the dashed line. Traces in dark blue or red are at high angles to the main principal stress. Reproduced from Figure C-1 in Follin (2008).

Inside fracture domain FFM01 (Figure 7), there are eight steeply dipping deformation zones that have two or more observations of transmissivity at different elevations (Figure 8). These zones are at a high angle to the main horizontal stress (Figure 5). The zones that have one or no observation of transmissivity are generally also at a high angle to the main horizontal stress. That is, inside FFM01 there are few zones that are parallel or sub-parallel to the main horizontal stress (Figure 7).

The transmissivity data of the eight zones with two or more transmissivity observations reveal substantial lateral hydraulic heterogeneity; the eight zones have different colours in Figure 8. Furthermore, transmissivity observations at shallow depths are in general of greater magnitude than values observed at large depths. Thus, there is both a similar lateral heterogeneity and a similar depth trend for the eight steeply dipping zones with two or more observations.

During the interference tests conducted in the upper 150 m of bedrock, see Follin et al. (2007b), the largest of the eight zones (ENE0060; not indicated in the figures shown here) revealed a hydraulic response at about 600-700 m. The hydraulic response was matched in the confirmatory step using a transmissivity model with an exponential depth trend and a lognormal distribution as model for lateral heterogeneity, see Follin et al. (2008) or Follin and Hartley (2013).

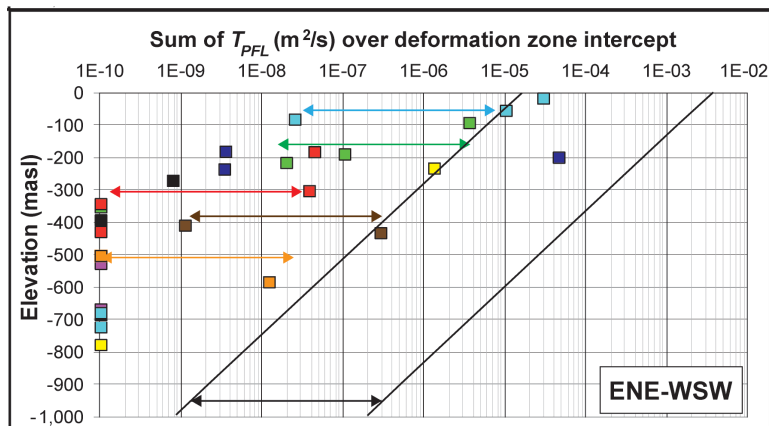


**Figure 8.** Inferred deformation zone transmissivity data ( $\Sigma T_{PFL}$ ) versus elevation of eight steeply dipping deformation zones with ENE–WSW strike that have two or more intercepts with transmissivity data, i.e., one colour per deformation zone. The two straight lines and the black double-head arrow show the inferred depth trend and lateral heterogeneity in deformation zone transmissivity of gently dipping deformation zones, see Follin and Stigsson (2013) for details.

*Consequence for SR-Site:* In conclusion, alternative transmissivity models were not developed in SDM-Site. Instead, focus was put on conditioning the propagated transmissivity model against measured data. The overall depth trend in transmissivity of deformation zones is based on an interpretation of site data of the observed decrease in maximum and geometric mean transmissivity with depth. This pattern is consistent with the expected sensitivity of effective hydraulic aperture to the increase of in situ stress with depth. There is also a large lateral heterogeneity in transmissivity, equating to a 95% confidence interval spanning 2.5 orders of magnitude. The same magnitude of variation in the geometric mean takes place over 600m of depth according to the interpreted trend, i.e. from the surface to below the repository, and so the realisations will create transmissivities at repository depth equal to those at the surface at some places in each realisation. The propagated model has been found to reproduce observed hydraulic responses at about 600-700 m depth during the conducted interference tests.

The ten realisations in SR-Site including lateral heterogeneity in the deformation zones could be considered a proxy for uncertainties in the depth trend also. Section 6.2.7 of (Joyce et al. 2010a) found little variability in median values of performance measures, but some variability in the high end tails of  $U_r$  and in the low end tails of  $F_r$  and  $t_{w,r}$ ; however, these were found to result from rare large stochastic fractures intersecting deposition holes rather than less favourable deformation zone properties. Hence, this uncertainty is considered less important than the intensity-size-transmissivity relations. Nonetheless, it is recognized that the development of appropriate criteria (including susceptibility to saline up-coning) for avoidance of large structures, identified deformation zones or otherwise, and especially ones with high specific capacity, is an important part of planning for underground construction and operations.

## 8. Sensitivity to intensity-scaling

*Comment/question:* SKB has only considered one of the Geo-DFN models within the Hydro-DFN modelling. Alternative Geo-DFN models recommended by Fox et al. (2007) include different relationships for different fracture size intensities, and a model with heterogeneous fracture intensity represented by a Gamma distribution.

## Response

It has been suggested (Dershowitz 1984) that, in the absence of other controlling factors such as lithology or deformation zones,  $P_{32}$  for a system exhibiting Euclidean scaling behaviour which follows a Poisson point process for fracture centres should follow a Gamma ( $\gamma$ ) distribution.

The stochastic intensity model studied by Fox et al. (2007) is built using power laws, and combines fracture intensity data of “all fractures” (i.e. broken and unbroken) from outcrops ( $P_{21}$ ) and cored boreholes ( $P_{10}$ ) to simultaneously match both data sets. Hence, fracture intensities are computed in terms of both sealed and open fractures; no distinction between the two classes is made in the Geo-DFN. Volumetric intensity statistics of “all fractures” ( $P_{32,a}$ ) are presented for each fracture set in three fracture domains (FFM01-FFM03), and the spatial variation of intensity described as a function of lithology or as a Gamma distribution (where possible).

In contrast, the Hydro-DFN model studied by Follin et al. (2007a) focuses on “open fractures” (i.e. broken fractures) from cored boreholes and flowing fractures detected with the PFL method in the same boreholes. Volumetric intensity statistics of open flowing fractures ( $P_{32,o}$  and  $P_{32,PFL}$ , respectively) are presented for each fracture set in all domains (FFM01-FFM06), and the spatial variation of intensity described as a function of depth (see Appendix C in Follin 2008 for details). This means that rather than using the Gamma distribution to describe the spatial variation of intensity, the Hydro-DFN model uses depth as a “controlling factor”. In operation, fracture domains FFM01 and FFM06 were divided into three sub-domains (“depth zones”) and fracture domains FFM03-05 into two depth zones. Fracture domain FFM02 was treated as a single depth zone.

In conclusion, the Hydro-DFN model developed for SDM-Site Forsmark suggests “global intensity values” according to fracture set, fracture domain and depth zone. The fracture intensity of each depth zone is regarded as homogeneous but may vary between fracture sets. Thus, the statistical matching (calibration) in the Hydro-DFN modelling was made against average intensity values. The average values were attained by pooling all fracture frequency data acquired in the cored boreholes drilled in each depth zone. Individual boreholes (and local sets) were not simulated.

It should be noted that Poissonian spatial structure for “open fractures” does not imply that the distribution of flow-conducting fractures also exhibits a Poissonian spatial structure, as fractal clustering of such fractures can arise spontaneously in a fracture system if it is close to the percolation threshold, see e.g. (Bour and Davy 1997, 1998, Follin et al. 2006, Appendix C). Furthermore, lack of connectivity implies that the intensity of flow-conducting fractures does not obey the principle of a tectonic continuum at all scales (Figure 9), see Appendix C in Follin (2008) and Section 4.5 of Hartley and Roberts (2013) for plots showing simulation results.

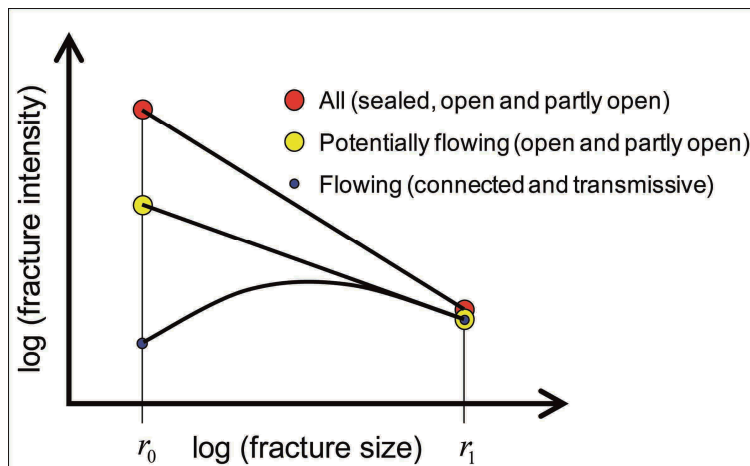


**Figure 9.** Envisaged relationship between the probability density functions of all, open, and flowing fractures for a power law fracture size probability density distribution

Consequence for SR-Site: Due to the huge decrease with depth of the intensity of flow conducting fractures detected by the PFL method it was not considered representative to adopt intensity-size concepts developed in the Geo-DFN, in which no depth trend in intensity was interpreted. The methodology used for interpretation of intensity-size scaling appropriate to the sub-set of open fractures had to be adapted to site conditions, principally focused on mimicking the observed drop in flow conducting fracture connectivity with depth. Supporting studies have demonstrated the non-Poissonian spatial distribution of connected open fractures that typically arises in sparse networks. Since observed flow conducting fractures above the PFL detection limit are extremely sparse and occur as single discrete features it is believed that uncertainties in intensity-size scaling relationships are of greater significance to safety assessment than the spatial model.

#### 9. Sensitivity to fracture sets and orientations and link to Geo-DFN versions

Comment/question: SKB applies statistical Geo-DFN models based on data freeze 1.2 as a basis for the Hydro-DFN calibration instead of Geo-DFN models based on data freeze 2.2 (Follin et al., 2007 p 155, second paragraph). In Follin et al. (2007 p 155, first paragraph) it is described how available data from data freeze 1.2 was confined to the target area, but how a significantly greater data amount became available in data freeze 2.2. Specifically, in the target area several inclined boreholes were drilled that provided a better indication of sub-vertical fracture formation and anisotropy. In addition, it is described how the Geo-DFN model based on data freeze 2.2 has limited implications on the results of the calibration study of the Hydro-DFN model 2.2. However, it remains unclear if this judgement has been assessed.

#### Response

The conceptual foundations for both geological and hydrogeological DFN models were consistent and remained unchanged throughout the site investigations (Munier et al. 2003, Munier 2004). Likewise, the geological and structural frameworks in terms of fracture domains and deformation zones (SKB 2006b, Olofsson et al. 2007) used in Stage 2.2 of the SDM were common to both Geo-DFN (Fox et al. 2007) and Hydro-DFN modelling for Stage 2.2. Additional specific details that the Hydro-DFN would ideally share with the Geo-DFN are the definition of fracture orientation sets, and

concepts for fracture spatial-scaling (discussed above) and size-scaling. Because of programme constraints on the SDM, the two models were developed in parallel with *a posteriori* checks that the Hydro-DFN model was not contrary to the Geo-DFN in terms of interpreted fracture sets and size concepts, in the sense that the modelled intensity of open fractures (as modelled by the Hydro-DFN) should be lower than that of all fractures (as modelled by the Geo-DFN) at all scales and for all fracture sets.

A difference between Geo-DFN Version 1.2 and 2.2 is that Version 2.2 introduced a number of local fracture sets on top the global sets defined in Version 1.2. Evidently, the local sets refer to local conditions. However, the Hydro-DFN model was aimed at describing overall site-scale conditions within each fracture domain. As described under the previous response, conditions in individual borehole were not modelled.

As noted above and on p. 155 of Follin et al. (2007a) the Geo-DFN model for Forsmark stage 2.2 treats all fractures, sealed as well as open, and mixes fractures gathered on outcrops with fractures gathered in boreholes. In contrast, the Hydro-DFN model focuses on open (and partly open) fractures gathered in cored boreholes below 100 m depth solely. Because of this difference in focus it is not necessarily appropriate that details such as orientations sets and fracture size models be identical. The relative models for orientation set are discussed here; fracture-size is discussed as part of the next issue.

The interpretation of fracture sets appropriate to the Hydro-DFN has typically been performed by analysis of stereonets of the open and water conducting fracture orientations. Generally the sets considered appropriate for water conducting fractures have been broadly consistent with those interpreted for all fractures in the Geo-DFN models. However, as shown in Figures 10-7 to 10-9 and Figure 10-17 of Follin et al. (2007a) the relative intensities and concentrations of orientations between sets can vary significant between all, open and PFL-f classes of fractures. Therefore, results are sensitive as to which class of fractures is used as the basis for interpreting orientation distributions. Differences in concentration of orientation within a set affect connectivity of the system. For this reason, in the Hydro-DFN it was considered more important that orientations should honour the observed distributions for the sub-set of PFL detected fractures than have a direct link to the Geo-DFN orientation model. The sensitivity to this decision was explored and found to have moderate importance at Forsmark. Two possible set definitions and orientation distributions were derived: one based on F1.2 Geo-DFN set definitions and an alternative (Follin et al. 2007a, Section 11.6) based on interpretation of the F2.2 borehole data. During the regional modelling for SDM-site (Follin et al. 2007b) higher concentration of orientation of the dominant sub-horizontal set implied by the alternative orientation model was found to be more representative of the high hydraulic anisotropy apparent when simulating interference tests and the palaeo-climatic evolution. Therefore, in SDM F2.3 (Follin et al. 2008) and in SR-Site (Joyce et al. 2010a) the alternative orientation model was used.

*Consequence for SR-Site: In the F2.2 Hydro-DFN modelling, the F1.2 definitions of fracture sets and orientation distributions were used. However, an alternative set definition and orientation distributions for open fractures were recommended in Chapter 11 of Follin et al. (2007a) and this was used in F2.3 and SR-Site. Based on the confirmatory tests performed in F2.2 it was found that this alternative orientation model could offer a better description of significant anisotropy evident in hydraulic interference tests and palaeo-climatic tests. The significant change with this alternative*

model was a higher Fisher concentration in the dominant sub-horizontal (SH) set, increased from 8.2 to 15.2 for FFM01. A similar change was made in Fisher concentration of the global SH set in F2.2 Geo-DFN, an increase to 17.4 in FFM01. The Fisher concentration of the other important set for hydrogeology, the NE set, was 14.3 in the Hydro-DFN and 20.9 in the Geo-DFN, i.e. both of high concentration. These parameters are the main orientation parameters that affect hydraulic connectivity and anisotropy, and they are similar between the Hydro-DFN used in SR-Site and the F2.2 Geo-DFN.

## 10. Sensitivity to size distribution parameters

*Comment/question: A number of steps and assumptions in the calibration of the Hydro-DFN model (Follin et al., 2007 p 175-195) results in the fact that the fitted parameters of the size distribution ( $r_0$  and  $k_r$ ) either are on the limit or outside the parameter space initially assumed. The parameter  $r_0$  was found to be at the lower limit of the assumed range 0.038 to 0.282. The calibrated values of  $k_r$  range from 2.4 for sub-horizontal fractures to 3.0 for NW and EW trending sets in fracture domains FFM01 and FFM02. This can be compared to the initially assumed span from 2.6 to 2.9. Follin et al., (2007 p 167, first paragraph) conclude that the fracture network's connectivity is very sensitive to the power-law size distribution applied in the Hydro-DFN model. The frequency of hydraulically connected fractures in the chosen alternative of fracture domain FFM01 is somewhat lower than that indicated by PFL measurements (Follin et al., 2007 p 170, Figure 11-8).*

### Response

At both Forsmark (Follin et al. 2007a) and Laxemar (Rhén et al. 2008), the observed intensity of open fractures recorded in core-drilled boreholes is much larger (even when restricted to certain and probable classifications) than the observed intensity of fractures carrying flow above the detection limit of the PFL-f method. The reasons that a hydraulically open part of a fracture might not carry flow above the PFL-f method detection limit (see Follin et al. 2011) include that:

- It is not connected to the percolating network, and so cannot carry flow;
- It has such low transmissivity that it cannot carry flow above the detection limit of the PFL-f method;
- Although the intersecting fracture itself might be highly transmissive locally, the percolating network that it is connected to has an effective transmissivity that is so low that it cannot supply the intersecting fracture with enough groundwater to allow an inflow above the detection limit of the PFL-f method.

Each cause above describes a constraint on groundwater flow, or flow bottleneck. The first cause describes a constraint based on fracture network connectivity, which is mainly determined by fracture intensity and size; the last two reasons describe different types of transmissivity bottlenecks. From borehole observations it is not possible to quantify what combination of these causes the apparent lack of flow communication seen in the PFL-f tests at Forsmark.

The ability of the distribution of transmissivity to cause hydraulic chokes and control apparent flow characteristics of a network as the mean transmissivity approaches the PFL detection limit has been demonstrated at SFR (see Öhman and Follin 2010).

As discussed in Point 2 above, the ability to achieve a lower detection limit for PFL-f tests in the ONKALO pilot holes at Olkiluoto has confirmed that flow bottlenecks due to the transmissivity distribution is certainly a factor affecting the apparent connectivity at depth at Olkiluoto. With a much lower detection limit, the Hydro-DFN parameterisation of intensity-size-transmissivity had to be changed markedly at depth toward shape parameters,  $k_r$ , about 2.4, with lower coefficients and high scaling exponents for size-transmissivity, but together these changes preserve the intensity-size distribution of connected open fractures above the original  $10^{-9}$  m<sup>2</sup>/s detection limit. This example illustrates an important point that the modelled intensity-size-transmissivity parameters can be very sensitive to the particular sub-set of fractures being modelled (i.e.  $P_{10,all} \geq P_{10,open} \geq P_{10,co} \geq P_{10,PFL}$ ) as discussed in Subsection 11.2.2 of Follin et al. (2007a). It is also recognised that it can be difficult to readily interpret the significance of the parameters of power-law formulation of intensity-size-transmissivity relationships and compare models on such basis. Perhaps it is more instructive to present and compare the size distribution of connected open fractures above certain transmissivity limits as shown in Figure 4-16 and Figure 4-17 in Hartley and Roberts (2013). Figure 4-16 is for Forsmark and demonstrates how very few fractures greater than c. 10m radius are connected below -400m, and so the size distribution used for small fractures has little relevance at this depth (see also Appendix C in Follin 2008). Figure 4-17 is for Laxemar and demonstrates that when different assumptions about the intensity and minimum size of open fractures were tested, the resulting size distribution for open connected fractures had similar characteristics.

The Hydro-DFN calibration method used at Forsmark considers constraints on flow to be caused predominately by the connectivity of the network of fractures with transmissivities above the detection limit c.  $10^{-9}$  m<sup>2</sup>/s. This assumption is implemented by equating the intensity of connected open fractures simulated, with the intensity of PFL-f fractures measured, that is, by equating the measured intensity of PFL-f fractures with a quantity simulated by purely geometrical specifications to calibrate appropriate power-law size parameters ( $r_0$ ,  $k_r$ ). Calibrating on connectivity in this way only provides one constraint, and so one of the size parameters has to be assumed and the other adjusted to match the observed connectivity.

This approach was at a formative stage at Forsmark (even at stage 2.2) and so the sensitivity to the size parameters was illustrated using four alternative *a priori* guesses at suitable parameters (see Subsection 11.4.1 of Follin et al. 2007a), the numbers chosen have no greater significance, but are based on previous works reported by La Pointe et al. (1999). Some results for these tests are presented in Figure 11-8 of Follin et al. (2007a) as mere illustrations of the sensitivity of connectivity to the size parameters for a sparse network such as Forsmark; however it is important to note these tests did not include the additional depth dependency in open and PFL fractures that was represented in the final Hydro-DFN. The only real significance of these test results was that it guided the assumption that  $r_0$  be set to 0.038m since the test cases with setting had come closest to the observation;  $k_r$  then became the connectivity matching parameter. The higher values of  $k_r$  used for the NW and EW set merely reflect the fact that no flow conducting fractures in these sets were detected by PFL in FFM01. In a sense these sets could have been eliminated from FFM01 altogether, but were retained with a nominal

high  $k_r$  to be conservative. By contrast, a lower value of  $k_r$  for the sub-horizontal set was required to increase the connectivity of this set as it was predicting too few PFL fractures for the KRMIN\_RMIN case shown in Figure 11-8 of Follin et al. (2007a).

As a final point on calibrated intensity-size distributions, perhaps relating more to the previous question, the models were checked for consistency with the models interpreted from the Geo-DFN modelling (Fox et al. 2007). Appendix C of Follin (2008) and Figure 4-12 of Hartley and Roberts (2013) shows the intensity-size distribution for the 3 depth zones developed in the Hydro-DFN modelling of FFM01/FFM06 along with that for FFM02, corresponding to the uppermost part of the bedrock in the candidate area. For all depths, the intensity-size distributions for open fractures are below the Geo-DFN, consistent with the concept that open fractures are everywhere a sub-set of all fractures.

*Consequence for SR-Site: There are not believed to be any inconsistencies in the calibration procedure followed for intensity-size scaling. Nonetheless, it is recognised that open fracture intensity-size relationships can have important implications for the detrimental tails of performance measures as exemplified by the stochastic simulation results of Subsection 6.2.7 of (Joyce et al. 2012a). Again, it is expected that significantly improved quantification of scaling relationships for the bedrock at depth can only practically be achieved by underground characterisation (e.g. tunnel mapping, correlating fractures between tunnels/pilot holes, and underground geophysical methods).*

#### 11. Sensitivity to stochastic sampling of Hydro-DFN

*Comment/question: Uncertainties relating to the stochastic formulation of the Hydro-DFN model and the stochastic properties of deformation zones have been addressed assessing ten realizations of the hydrogeological models on regional and local scales (Joyce et al., p 63 and 65). Due to a request by the NEA's international reviewers, SKB has performed additional realizations to support the NEA's purposes. The limited number of realizations is based on the long execution times of the models. The variability between realizations has been discussed in the form of statistics of performance measures calculated using particle tracking. The results indicate that these measures can be sensitive to variations in the stochastic geometry and properties between realizations (Joyce et al., 2010 p 94-96).*

#### Response

The peak risk calculated in SR-Site increases close to linearly with the number of failed canisters. In the review of SR-Site conducted by NEA, a question was posed if the mean number of failed canisters is sensitive to the number of performed realizations in the hydrogeological modelling. In the answer (Hedin 2011) to NEA, it was concluded that additional realizations would have a very small effect on the expected number of failed canisters. In the analyses, the distribution of failed canisters was assumed to be either normal or log-normal; in both cases it was shown that the upper 95% confidence interval was approximately a factor of 2 (for the correlated case used in the compliance calculations) larger than the mean value of the normal and log-normal distributions. These results were later confirmed by additional numerical simulations performed (Hedin 2012). In short, 15 additional realizations of the correlated case were performed, and using these results the mean number of failed canisters (over 20 realizations) was just marginally changed. However, the 95% confidence limit was substantially reduced;

specifically, the upper 95% confidence limit was now just a factor of approximately 1.2 larger than the mean value of the normal and log-normal distributions, respectively.

Whether a canister fails or not is related to the magnitude of groundwater flow (Darcy flux) in the fracture(s) intersecting a deposition hole. The analysis described above thus strictly only addresses the issue of whether a sufficient number of realizations have been used to capture a robust estimate of the expected number of failed canisters (and hence groundwater flow at deposition hole locations). The analysis does however not strictly address the issue how the statistics of travel time and flow-related transport resistance (F), obtained through particle tracking, could be affected by additional realizations. In Joyce et al. (2010), Figure 6-17 (CDF plots) and 6-18 (bar-and-whisker plots), ten realizations of the Hydro-DFN model (semi-correlated fracture size-transmissivity) and ten realizations of the deformation zone model are combined into ten realizations of the groundwater flow model. The variability in travel time and F distributions appear to be somewhat larger between realizations than the corresponding variability in Darcy flux. However, we note the following:

- We have, with the analyses reported to the NEA, demonstrated that we have a sufficient number of model realisations to obtain a reliable characterisation of the high-end tail of the distribution of Darcy fluxes at deposition hole positions, i. e. the entity that determines the number of failed canisters and which hence is the primary entity in the determination of risk.
- Due to the correlation between high Darcy fluxes and low F values, this also means that deposition hole positions associated with low F values will be “selected” and propagated to the further calculation of radionuclide transport and hence risk.
- That also the predominantly low-end part of the F distribution is sufficiently well sampled with the number of realisations used in SR-Site (and the additional realisations in the further analyses reported to the NEA) can strictly be addressed by e.g. extending the NEA-analyses to a full risk calculation. However, as evidenced by e.g. Figures 13-39 and 13-40 in SKB (2011), the overall reduction of risk due to geosphere retention is less than a factor of 10, meaning that the possible impact on risk by additional realisations is deemed to be minor.

*Consequence for SR-Site: SKB concludes that the uncertainty related to number of realizations of the hydrogeological model (Hydro-DFN model and deformation zone model) is small relative to other uncertainties discussed in this memo.*

## 12. Sensitivity to domain size used in Hydro-DFN model calibration

*Comment/question: SKB chooses a certain domain size in the Hydro-DFN calibration when calculating the frequency of fractures having connections to the model boundaries and that intersect a simulated borehole. The domain size in the simulation is set at 400 m in the horizontal direction based on the average distance between sub-vertical deformation zones (Follin et al., 2007 p 165). The boreholes at the site do, however, have varying distances to their closest deformation zone, and these deformation zones could be effective hydraulic barriers during PFL measurements. The choice of a certain, constant, distance between the simulated borehole and the boundary in the*

*simulations can be expected to affect the frequency of connected fractures for a given parameter set, and hence also for the parameter calibration.*

### Response

In the connectivity calculations of the Forsmark Hydro-DFN a domain size of 400m horizontally was used surrounding a synthetic vertical borehole in the centre of the domain and being 1000m long (see Subsection 11.4.1 of Follin et al. 2007a). The choice of domain size was based on the approximate average spacing of deformation zones within the local scale geological modelling area. No deformation zones were included in the models used to calibrate the Hydro-DFN model. The same approach was used in the Hydro-DFN model developed for the Laxemar SDM (Rhén et al. 2008). It was then straightforward to compare statistics of fracture intensity and specific flow capacity from stochastic simulations for the synthetic borehole with equivalent statistics for each fracture domain and depth zones. Whether the calibration of fracture-size and transmissivity might be sensitive to the choice of domain size was not tested as part of the SDM-Site modelling. A significantly larger size of the model domain than the one used, with no intersecting deterministic deformation zones in between the borehole and the boundaries, might render a different power law size distribution with a low value of the shape parameter. However, such a scenario is doubtful considering the frequency of the deformation zone model derived for Forsmark (cf. Figure 7).

However, as part of the comparisons made between Laxemar and Forsmark in support of SR-Site (Joyce et al. 2010b, Appendix E), the influence of deformation zones on Hydro-DFN model calibration was examined. This was part of a wider investigation of whether aspects of the calibration methodology or assumptions used in SDM-Site Laxemar (Rhén et al. 2008) could potentially lead to either over-estimating the number of large conductive fractures (corresponding to an under-estimate of the power-law exponent,  $k_r$ , in the fracture size distribution) or over-estimating the transmissivity of fractures; since the Laxemar Hydro-DFN seemed to be predicting a system slightly too conductive (c. factor 3) according to the confirmatory testing. As a result the Hydro-DFN methodology was elaborated in a number of ways. Of relevance here was the change to using a selection of actual boreholes modelled in their true locations and orientations and with deformation zones included in the stochastic Hydro-DFN model calibration (see Figures 5-1 and 5-2 of Joyce et al. 2010b). For each fracture domain, an appropriate set of boreholes were selected that are representative of the domain in terms of having the majority of its length in the domain and extending to at least repository depth within the domain. The significance of this change is that specific deformation zones are effectively controlling the distance from the representative borehole to a specified pressure boundary condition. Since the actual deformation zones are sometimes closer than the model boundary to the representative boreholes, and probably more importantly can also intersect them creating local clusters of connected fractures around them (a situation not allowed for in the idealised case), the calibrated fracture size distribution was found to be shifted slightly towards smaller fractures compared to the original SDM calibration method which did not include deformation zones explicitly.

This same elaborated methodology was included as part of the Olkiluoto SDM 2011 (Hartley et al. 2012a). Again, the earlier 2008 SDM (Hartley et al. 2009) that used the same calibration methodology as for the Forsmark SDM with simulated synthetic vertical boreholes without deformation zones lead to a slightly overly conductive

system as indicated by confirmatory tests such as against hydrogeochemistry data. By calibrating the Hydro-DFN update with deformation zones included, and some other methodology changes, then the fracture size distribution was shifted towards fewer large stochastic fractures created in the Hydro-DFN model. The consequence was a hydrogeological parameterisation better able to simulate observed site conditions.

The sensitivity of the Forsmark Hydro-DFN to the change in methodology described above has not been quantified. At Laxemar and Olkiluoto the change in methodology resulted in slightly fewer large stochastic fractures. It is repeated, however, that a key characteristic of the crystalline bedrock at Forsmark is the extremely low conductive fracture frequency at repository depth. At Laxemar and Olkiluoto the conductive fracture frequency at repository depth is higher, in particular at Laxemar.

*Consequence for SR-Site: Experiences from a more elaborate Hydro-DFN model calibration approach simulating individual borehole conditions including deformation zones for Laxemar and Olkiluoto were both found to result in shifts toward slightly fewer large stochastic fractures, since the deformation zones increased connectivity and sometimes were located nearer to a fixed head boundary. It has not been quantified whether a similar methodology applied to the Forsmark Hydro-DFN would have any beneficial effects on the safety assessment resulting from fewer large stochastic fractures cutting deposition tunnels and holes.*

## References

- Ahokas H, Pöllänen J, Rouhiainen, P, Kuusela-Lahtinen A, 2013.** Quality review of transmissivity data from olkiluoto Site – Drillholes OL-KR1–KR57. Posiva Working Report 2012-99, Posiva Oy, Finland
- Black J H, Barker J A, Woodman N D, 2007.** An investigation of ‘sparse channel networks’: Characteristic behaviours and their causes. SKB R-07-35, Svensk Kärnbränslehantering AB.
- Bour O, Davy P, 1997.** Connectivity of random fault networks following a power law fault length distribution. *Water Resources Research* 33, 1567–1583.
- Bour O, Davy P, 1998.** On the connectivity of three-dimensional fault networks. *Water Resources Research* 34, 2611–2622.
- de Dreuzy J-R, Davy P, Bour O, 2000.** Percolation parameter and percolation-threshold estimates for three-dimensional random ellipses with widely scattered distributions of eccentricity and size. *Physical Review E* 62, 5948–5952.
- Dershowitz W, 1984.** Rock joint systems. PhD thesis. Massachusetts Institute of Technology, Cambridge, MA.
- Follin S, 2008.** Bedrock hydrogeology Forsmark. Site-descriptive modelling, SDM-Site Forsmark. SKB R-08-95, Svensk Kärnbränslehantering AB.
- Follin S, Hartley L, 2013.** Approaches to confirmatory testing of a groundwater flow model for sparsely fractured crystalline rock, exemplified by data from the proposed high-level nuclear waste repository site at Forsmark, Sweden. *Hydrogeology Journal*. doi:10.1007/s10040-013-1079-8
- Follin S, Stigsson M, 2013.** A transmissivity model for deformation zones in fractured crystalline rock and its possible correlation to in situ stress at the proposed high-level nuclear waste repository site at Forsmark, Sweden. *Hydrogeology Journal*. doi:10.1007/s10040-013-1078-9
- Follin S, Stigsson M, Svensson U, 2005.** Regional hydrogeological simulations for Forsmark – numerical modelling using DarcyTools. Preliminary site description Forsmark area – version 1.2. SKB R-05-60, Svensk Kärnbränslehantering AB.
- Follin S, Stigsson M, Svensson U, 2006.** Hydrogeological DFN modelling using structural and hydraulic data from KLX04. Preliminary site description Laxemar subarea - version 1.2. SKB R-06-24, Svensk Kärnbränslehantering AB
- Follin S, Levén J, Hartley L, Jackson P, Joyce S, Roberts D, Swift B, 2007a.** Hydrogeological characterisation and modelling of deformation zones and fracture domains, Forsmark modelling stage 2.2. SKB R-07-48, Svensk Kärnbränslehantering AB.
- Follin S, Johansson P-O, Hartley L, Jackson P, Roberts D, Marsic N, 2007b.** Hydrogeological conceptual model development and numerical modelling using

CONNECTFLOW, Forsmark modelling stage 2.2. SKB R-07-49, Svensk Kärnbränslehantering AB.

**Follin S, Hartley L, Jackson P, Roberts D, Marsic N, 2008.** Hydrogeological conceptual model development and numerical modelling using CONNECTFLOW, Forsmark modelling stage 2.3. SKB R-08-23, Svensk Kärnbränslehantering AB.

**Follin S, Ludvigson J-E, Levén J, 2011.** A comparison between standard well test evaluation methods used in SKB's site investigations and the generalised radial flow concept. SKB P-06-54, Svensk Kärnbränslehantering AB.

**Follin S, Hartley L, Rhén I, Jackson P, Joyce S, Roberts D, Swift B, 2013.** A methodology to constrain the parameters of a hydrogeological discrete fracture network model for sparsely fractured crystalline rock, exemplified by data from the proposed high-level nuclear waste repository site at Forsmark, Sweden. *Hydrogeology Journal*. doi:10.1007/s10040-013-1080-2

**Fox A, La Pointe P, Hermanson J, Öhman J, 2007.** Statistical geological discrete fracture network model. Forsmark modelling stage 2.2. SKB R-07-46, Svensk Kärnbränslehantering AB.

**Glamheden R, Fredriksson A, Röshoff K, Karlsson J, Hakami H, Christiansson R, 2007.** Rock mechanics Forsmark. Site descriptive modeling Forsmark stage 2.2. SKB R-07-31, Svensk Kärnbränslehantering AB.

**Hartley L, Joyce S, 2013.** Approaches and algorithms for groundwater flow modeling in support of site investigations and safety assessment of the Forsmark site, Sweden. *Journal of Hydrology* 500, 200–216.

**Hartley L, Roberts D, 2013.** Summary of discrete fracture network modelling as applied to hydrogeology of the Forsmark and Laxemar sites. SKB R-12-04, Svensk Kärnbränslehantering AB.

**Hartley L, Cox I, Hunter F, Jackson P, Joyce S, Swift B, Gylling B, Marsic N, 2005.** Regional hydrogeological simulations for Forsmark – numerical modelling using CONNECTFLOW. Preliminary site description Forsmark area – version 1.2. SKB R-05-32, Svensk Kärnbränslehantering AB.

**Hartley L, Hoch A, Jackson P, Joyce S, McCarthy R, Rodwell W, Swift B, Marsic N, 2006.** Groundwater flow and transport modelling during the temperate period for the SR-Can assessment. Forsmark area – version 1.2. SKB R-06-98, Svensk Kärnbränslehantering AB.

**Hartley L, Hoek J, Swan D, Roberts D, Joyce D, Follin S, 2009.** Development of a hydrogeological discrete fracture network model for the Olkiluoto site descriptive model 2008. Posiva Working Report 2009-61, Posiva Oy, Finland.

**Hartley L, Appleyard P, Baxter S, Hoek J, Roberts D, Swan S, 2012a.** Development of a hydrogeological discrete fracture network model for the Olkiluoto site descriptive model 2011. Posiva Working report 2012-32, Posiva Oy, Finland.

**Hartley L, Hoek J, Swan D, Appleyard P, Baxter S, Roberts D, Simpson T, 2012b.** Hydrogeological modelling for assessment of radionuclide release scenarios for the repository system 2012. Posiva Working Report 2012-42, Posiva Oy, Finland.

- Joyce S, Simpson T, Hartley L, Applegate D, Hoek J, Jackson P, Swan D, Marsic N, Follin S, 2010a.** Groundwater flow modelling of periods with temperate climate conditions – Forsmark. SKB R-09-20, Svensk Kärnbränslehantering AB.
- Joyce S, Simpson T, Hartley L, Applegate D, Hoek J, Jackson P, Roberts D, Swan D, Gylling B, Marsic N, Rhén I, 2010b.** Groundwater flow modelling of periods with temperate climate conditions – Laxemar. SKB R-09-24, Svensk Kärnbränslehantering AB.
- La Pointe P R, Cladouhos T, Follin S 1999.** Calculation of displacement on fractures intersecting canisters induced by earthquakes: Aberg, Beberg and Ceberg examples. SKB TR-99-03, Svensk Kärnbränslehantering AB.
- Ludvigson J-E, Hansson K, Rouhiainen P, 2002.** Methodology study of Posiva difference flow meter in borehole KLX02 at Laxemar. SKB R-01-52, Svensk Kärnbränslehantering AB.
- Ludvigson J-E, Hansson K, Hjerne C, 2007.** Forsmark site investigation. Method evaluation of single-hole hydraulic injection tests at site investigations in Forsmark. SKB P-07-80, Svensk Kärnbränslehantering AB.
- Martin C D, 2007.** Quantifying in situ stress magnitudes and orientations for Forsmark. Forsmark stage 2.2. SKB R-07-26, Svensk Kärnbränslehantering AB.
- Mattila J, Tammisto E, 2012.** Stress-controlled fluid flow in fractures at the site of a potential nuclear waste repository, Finland. *Geology* 40, 299–302.
- Mourzenko V V, Thovert J F, Adler P M, 2004.** Macroscopic permeability of three-dimensional fracture networks with a power-law size distribution. *Physical Review E* 69, 066307.
- Mourzenko V V, Thovert J F, Adler P M, 2005.** Percolation of three-dimensional fracture networks with power-law size distribution. *Physical Review E* 72, 036103.
- Munier R, 2004.** Statistical analysis of fracture data, adapted for modelling discrete fracture networks – Version 2. SKB R-04-66, Svensk Kärnbränslehantering AB.
- Munier R, Stenberg L, Stanfors R, Milnes A G, J Hermanson, Triumf C-A, 2003.** Geological Site Descriptive Model. A strategy for the model development during site investigations. SKB R-03-07, Svensk Kärnbränslehantering AB.
- Olofsson I, Simeonov A, Stephens M, Follin S, Nilsson A-C, Röshoff K, Lindberg U, Lanaro F, Fredriksson A, Persson L, 2007.** Site descriptive modelling Forsmark, stage 2.2. A fracture domain concept as a basis for the statistical modelling of fractures and minor deformation zones, and interdisciplinary coordination. SKB R-07-15, Svensk Kärnbränslehantering AB.
- Painter S, 2006.** Effect of single-fracture aperture variability on field-scale transport. SKB R-06-25, Svensk Kärnbränslehantering AB.
- Pöllänen J, Sokolnicki M, 2004.** Forsmark site investigation. Difference flow logging of borehole KFM03A, SKB P-04-189, Svensk Kärnbränslehantering AB.

**Rhén I, Forsmark T, Hartley L, Jackson P, Roberts D, Swan D, Gylling B, 2008.** Hydrogeological conceptualisation and parameterisation. Site descriptive modelling, SDM-Site Laxemar. SKB R-08-78, Svensk Kärnbränslehantering AB.

**Rouhiainen P, Pöllänen J, 2003.** Forsmark site investigation. Difference flow logging of borehole KFM01A, SKB P-03-28, Svensk Kärnbränslehantering AB.

**Salas J, Gimeno M J, Auqué L, Molinero J, Gómez J, Juárez I, 2010.** SR-Site – hydrogeochemical evolution of the Forsmark site. SKB TR-10-58, Svensk Kärnbränslehantering AB.

**Selroos J-O, Follin S, 2010.** SR-Site groundwater flow modelling methodology, setup and results. SKB R-09-22, Svensk Kärnbränslehantering AB.

**SKB, 2006a.** Long-term safety for KBS-3 repositories at Forsmark and Laxemar – a first evaluation. Main report of the SR-Can project. SKB TR-06-09, Svensk Kärnbränslehantering AB.

**SKB, 2006b.** Site descriptive modelling Forsmark stage 2.1. Feedback for completion of the site investigation including input from safety assessment and repository engineering. SKB R-06-38, Svensk Kärnbränslehantering AB.

**SKB, 2008.** Site description of Forsmark at completion of the site investigation phase. SDM-Site Forsmark. SKB TR-08-05, Svensk Kärnbränslehantering AB.

**SKB, 2010.** Fud-program 2010. Program för forskning, utveckling och demonstration av metoder för hantering och slutförvaring av kärnavfall. Svensk Kärnbränslehantering AB.

**SKB, 2011.** Long-term safety for the final repository for spent nuclear fuel at Forsmark. Main report of the SR-Site project, Volume III. SKB TR-11-01, Svensk Kärnbränslehantering AB.

**Stephens M B, Fox A, La Pointe P, Simeonov A, Isaksson H, Hermanson J, Öhman J, 2007.** Geology Forsmark. Site descriptive modelling, Forsmark stage 2.2, SKB R-07-45, Svensk Kärnbränslehantering AB.

**Svensson U, Follin S, 2010.** Groundwater flow modelling of the excavation and operational phases – Forsmark. SKB R-09-19, Svensk Kärnbränslehantering AB.

**Terzaghi R D, 1965.** Sources of error in joint surveys. *Géotechnique* 15, 287–304.

**Vidstrand P, Follin S, Zugec N, 2010.** Groundwater flow modelling of periods with periglacial and glacial climate conditions – Forsmark. SKB R-09-21, Svensk Kärnbränslehantering AB.

**Öhman J, Follin S, 2010.** Site investigation SFR. Hydrogeological modelling of SFR. Model version 0.2. SKB R-10-03, Svensk Kärnbränslehantering AB.

#### **Unpublished documents:**

**Hedin A, 2011.** Additional information requested by the IRT at December hearings. SKBdoc 1323497 ver 1.0, Svensk Kärnbränslehantering AB.

**Hedin A, 2012.** Additional hydrogeological model realisations. SKBdoc 1343309 ver 1.0, Svensk Kärnbränslehantering AB.